Chinese Chemical Letters 33 (2022) 3061–3064

Contents lists available at ScienceDirect

Chinese Chemical Letters

journal homepage: www.elsevier.com/locate/cclet

Semi-chemical interaction between graphitic carbon nitride and Pt for boosting photocatalytic hydrogen evolution

Ziai Zhong[a,1], Lisha Chen[a,c,1], Longshuai Zhang[a,*], Feiyao Wu[a], Xunheng Jiang[a], Haiyan Liu[a], Fengrong Lv[a], Haiyang Xie[a], Fanqi Meng[b], Lingling Zheng[a,c], Jianping Zou[a,*]

[a] Key Laboratory of Jiangxi Province for Persistent Pollutants Control and Resources Recycle, Nanchang Hangkong University, Nanchang 330063, China
[b] State Key Laboratory of New Ceramics and Fine Processing, School of Materials Science and Engineering, Tsinghua University, Beijing 100084, China
[c] Key Laboratory of Poyang Lake Environment and Resource Utilization of Ministry of Education, School of Resources Environmental and Chemical Engineering, Nanchang University, Nanchang 330031, China

ARTICLE INFO

Article history:
Received 13 July 2021
Revised 15 August 2021
Accepted 16 September 2021
Available online 23 September 2021

Keywords:
Co-catalyst
Graphitic carbon nitride
H_2 evolution
Photocatalysis
Semi-chemical interaction

ABSTRACT

Owing to the exorbitant overpotential and serious carrier recombination of graphitic carbon nitride (g-C_3N_4), noble metal (NM) is usually served as the H_2 evolution co-catalyst. Although the NM (such as Pt) nanoparticles can reduce the H_2 evolution overpotential, the weak van der Waals interaction between Pt and g-C_3N_4 makes against the charge transfer. Herein, the solvothermal method is developed to achieve semi-chemical interaction between Pt and g-C_3N_4 nanotube (Pt-CNNT) for fast charge transfer. Moreover, the generated in-plane homojunction of CNNT can accelerate charge separation and restrain recombination. Meanwhile, the metallic Pt is an excellent H_2 evolution co-catalyst. Photo/electrochemical tests verify that the semi-chemical interaction can improve photogenerated charge separation and transferability of CNNT. As a result, the photocatalytic H_2 evolution turnover frequency (TOF) of Pt-CNNT under visible light irradiation reaches up to 918 h^{-1}, which is one of the highest in the g-C_3N_4-based photocatalysts. This work provides a new idea to improve the charge transfer for efficient photocatalytic H_2 evolution.

Solar energy to chemical energy conversion by photocatalytic water splitting was considered to be an effective program for solving the energy crisis and environmental pollution. Many photocatalysts were developed for efficient photocatalytic H_2 evolution [1–5]. Among them, graphitic carbon nitride (g-C_3N_4) has been studied extensively for solar energy to H_2, due to the visible light response, metal-free property, low price and so on [6–8]. However, the exorbitant overpotential and serious carrier recombination of g-C_3N_4 make the noble metal (NM) co-catalyst (such as Pt, Au) is necessary for efficient photocatalytic H_2 evolution reaction [9–11]. Although the co-catalyst could reduce overpotential for H_2 evolution, the weak van der Waals interaction between co-catalysts and photocatalysts impedes charge transfer and serves as recombination centers [12]. Therefore, enhancing the interaction between co-catalysts and g-C_3N_4 to accelerate charge transfer will benefit photocatalytic activity.

Unquestionably, the loading methods of co-catalysts have a great influence on the interaction between co-catalysts and photocatalysts [13]. *In situ* photo-reduction was the most common and simple method for NM nanoparticles (NPs) deposition, which could selectively load on the reduction sites for NM NPs [14,15]. In addition, chemical reduction was also used for the loading of NM NPs. The excellent dispersity and small sizes of NM NPs could provide more active sites [16]. Furthermore, the electrostatic interaction method was used to loading the prefab co-catalysts on the photocatalysts, which could adjust the sizes and morphology of co-catalysts rather than only the NPs [17,18]. However, all of these methods loaded NM co-catalysts showed the weak van der Waals interaction with the photocatalysts. Of course, there were also some studies about the strong interaction between co-catalysts and photocatalysts. The Pt^{4+} absorption and thermal reduction two-step method was used to prepare the Pt single atom decorated g-C_3N_4 by Pt-N coordination, which increased the lifetime of photogenerated electrons *via* changing the surface trap states [19]. In addition, the simple solution adsorption of Pt^{4+} also achieved the Pt-N coordination on g-C_3N_4, where the strong interaction between Pt and g-C_3N_4 could adjust the electronic structure of g-C_3N_4 and accelerate the charge transfer [20]. Although the strong interaction could accelerate charge transfer, the experiment and density functional theory (DFT) calculation indicated that the Pt in ionic state

* Corresponding authors.
E-mail addresses: L_S_Zhang1990@163.com (L. Zhang), zjp_112@126.com (J. Zou).
[1] These authors contributed equally to this work.

https://doi.org/10.1016/j.cclet.2021.09.057
1001-8417/

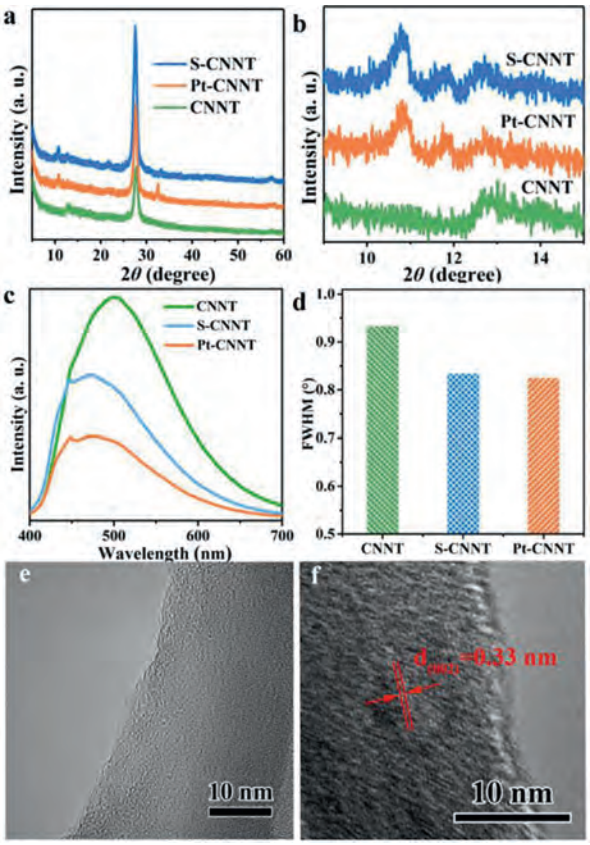

Fig. 1. (a, b) XRD patterns, (c) PL spectra and (d) FWHM of (002) peak of CNNT, S-CNNT and Pt-CNNT; HR-TEM images of (e) CNNT and (f) Pt-CNNT.

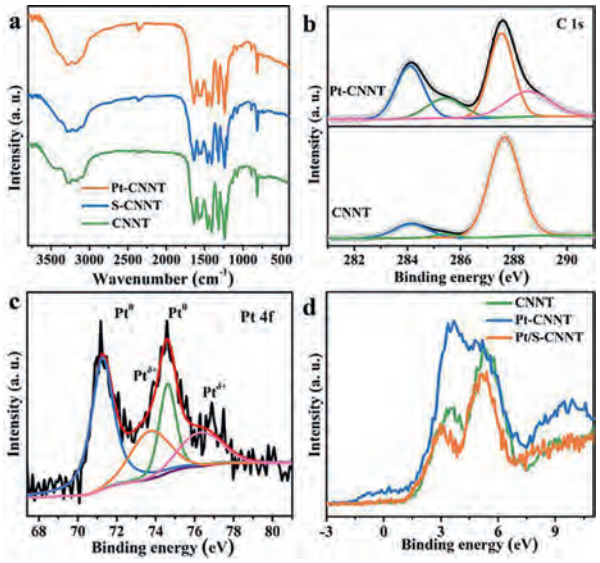

Fig. 2. (a) FT-IR spectra of CNNT, S-CNNT and Pt-CNNT, (b) C 1s spectra of CNNT and Pt-CNNT, (c) Pt 4f spectrum of Pt-CNNT, and (d) valance spectra of CNNT, Pt/S-CNNT and Pt-CNNT.

showed poor H_2 evolution activity than metallic Pt [21]. Therefore, it is anticipated to make the semi-chemical interaction between Pt and g-C_3N_4, where a part of Pt atoms has strong interaction with the g-C_3N_4 for fast charge transfer as well as the rest of metallic Pt is used for efficient H^+ reduction.

Herein, a solvothermal method was developed to prepare the Pt-g-C_3N_4 nanotube (Pt-CNNT) with the semi-chemical interaction between Pt and g-C_3N_4 nanotube (CNNT). X-ray diffraction (XRD), photoluminescence (PL), and high-resolution transmission electron microscopy (HR-TEM) proved the improved crystallinity and generated in-plane homojunction of CNNT, which could increase the photogenerated charge separation and migration. X-ray photoelectron spectroscopy (XPS) of Pt and valance band spectra of Pt-CNNT verified the semi-chemical interaction between Pt and CNNT, which can improve the photogenerated charge transfer from CNNT to Pt. And, photoelectricity tests showed the improved photogenerated charge transfer and migration ability of Pt-CNNT. As a result, the optimized Pt-CNNT showed an ultrahigh turnover frequency (TOF) for photocatalytic H_2 evolution.

As shown in Fig. 1a, CNNT had two XRD peaks center at 12.7° and 27.8°, corresponding to the (100) and (002) planes of g-C_3N_4, respectively [22,23]. However, after solvothermal treatment, the crystal structure of CNNT had obvious change. For S-CNNT (CNNT after solvothermal but without Pt) and Pt-CNNT, there were two new XRD peaks appeared at the left of (100) peak, located at 10.8° and 11.8°, respectively. Both of them are also (100) peaks similar to the peak located at 12.7° (Fig. 1b) [24]. The three clear (100) peaks indicated that the three in-plane repeat units had different widths (corresponding to d spaces of 0.819, 0.750 and 0.697 nm, respectively), which were caused by different crook degrees of the in-plane network [25]. According to XRD results, the possible structure mode of S-CNNT was proposed in Fig. S1 (Supporting information). Previous experimental and theoretical calculations certified that the different in-plane units crook could form discriminating energy levels structures [25,26]. As illustrated in Fig. 1c, CNNT revealed one PL peak centered at 500 nm. After the solvothermal process, this peak become less apparent and two new peaks appeared, centered at 475 and 440 nm, respectively. The three PL peaks of S-CNNT and Pt-CNNT indicated the three different bandgaps from the different in-plane units, which are consistent with the XRD results. Naturally, different bandgaps of S-CNNT and Pt-CNNT will cause different conduction band and valance band levels, hence, both of them would form in-plane homojunction, which can accelerate the charge separation and migration just like the heterojunctions [25]. The stronger PL quenching of S-CNNT and Pt-CNNT proves the in-plane homojunction could suppress the photogenerated charge recombination (Fig. 1c). In addition, the solvothermal could also increase the crystallinity of CNNT: first, in Fig. 1a, the emerged XRD peak at 32.5° of Pt-CNNT, belong to the (200) peak of g-C_3N_4 (JCPDS No. 78-1691); second, in Fig. 1d, S-CNNT and Pt-CNNT showed obvious reduced XRD full width at half maximum (FWHM) of (002) peak; third, in Figs. 1e and f, the HR-TEM images of CNNT showed no lattice fringe, but Pt-CNNT exhibited clear lattice fringes. All of these proved the solvothermal process could improve the crystallinity of CNNT.

Although the in-plane units of CNNT had been changed, the solvothermal treatment had no influence on the two-dimension layered texture of g-C_3N_4 (Fig. 1a). As shown in Fig. 2a, triazine ring breathing mode (807 cm^{-1}), various C–N and C=N stretches (1200–1600 cm^{-1}) and broad stretching modes of residual amino and possible hydroxyl (3100–3400 cm^{-1}) had no change after solvothermal. That is, the solvothermal treatment had no obvious influence on the matrix of g-C_3N_4 [27]. In addition, S-CNNT still exhibited a tubular morphology, similar to that of CNNT (Figs. S2 and S3 in Supporting information). Then, the chemical environment of Pt-CNNT was represented by XPS (Fig. S4a in Supporting information). In Fig. 2b, the C 1s XPS spectrum of CNNT can be divided into three peaks centered at 284.6, 285.9 and 288.0 eV, assigned to the standard reference carbon, C–O, and sp^2-bonded carbon (N–C=N), respectively. In addition, the C 1s spectrum of Pt-CNNT emerged a new peak centered at 289.1 eV, assigned to the carbon $\pi-\pi^*$ transition, which was due to the enhanced conju-

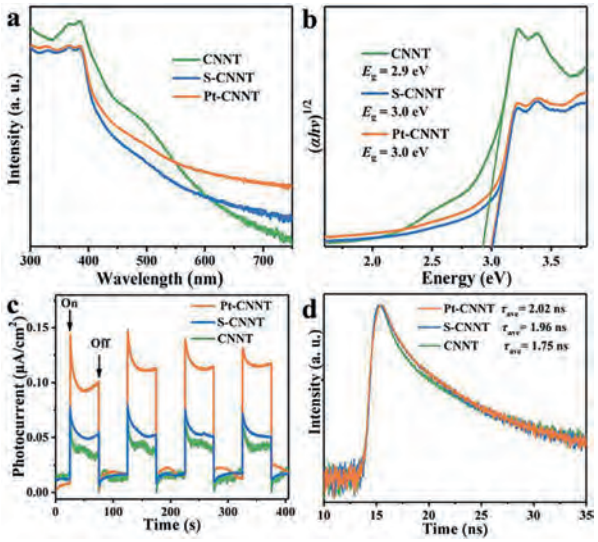

Fig. 3. (a) UV-vis absorption spectra, (b) Tacu plot, (c) photocurrent, and (d) time-resolved PL spectra of CNNT, S-CNNT and Pt-CNNT.

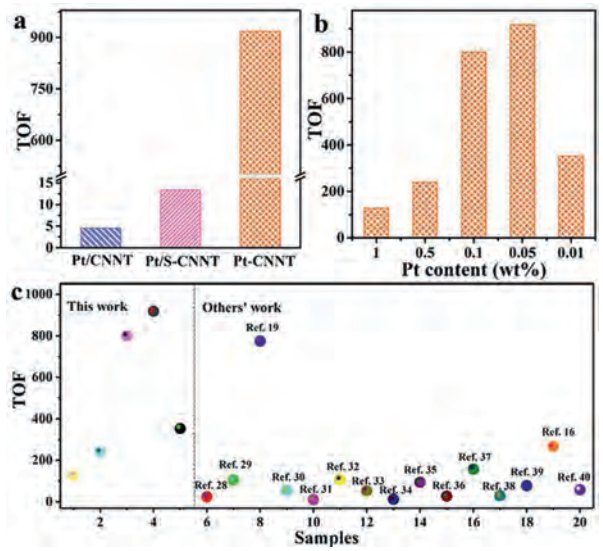

Fig. 4. H_2 evolution TOF of (a) Pt/CNNT, Pt/S-CNNT and Pt-CNNT, (b) different Pt content and (c) the typical g-C_3N_4-based photocatalysts.

gation arising from the more flat in-plane units [25]. In Fig. S4b (Supporting information), the broad peak of XPS N 1s spectrum can be deconvolved into three peaks located at 398.8, 400.2 and 401.3 eV, which corresponding to sp^2-hybridized nitrogen in the triazine ring (C–N=C), tertiary nitrogen (N–$(C)_3$), and amine groups (C–N–H), respectively [7]. After solvothermal treatment, the O content increased from 1.38 at% to 9.85 at% (Fig. S4c in Supporting information). High resolution XPS spectra of O 1s testified there was only one valance state of it. In addition, combine with the C 1s XPS spectrum of Pt-CNNT, O element was bonded with C.

As illustrated in Fig. 2c, the Pt 4f spectrum of Pt-CNNT could be divided into four peaks, centered at 71.3, 74.6, 73.8 and 76.3 eV, respectively. Two of them belonged to Pt $4f_{5/2}$ and Pt $4f_{7/2}$ of Pt^0 state, and the other two were assigned to Pt $4f_{5/2}$ and Pt $4f_{7/2}$ of $Pt^{\delta+}$ state, respectively [16,20]. As mentioned above, the O element in Pt-CNNT was bonded with C and no other chemical state, so, the $Pt^{\delta+}$ state was derived from the strong interaction between Pt and CNNT rather than Pt-O bond. In addition, density of states of Pt/S-CNNT's valance spectrum had no obvious difference compared with CNNT, indicate solvothermal treatment and photodeposition Pt had no influence on density of states of CNNT (Fig. 2d). However, Pt-CNNT showed obvious enhanced density of states between −1.5 eV and 1.5 eV, indicating the valence electron of Pt was transferred to CNNT due to the semi-chemical interaction of Pt and CNNT. The XPS results of Pt 4f and valance band spectra certified the strong interaction between Pt and CNNT.

In Fig. 3a, compared with CNNT, the light absorption of Pt-CNNT and S-CNNT showed an obvious blue shift, and the bandgaps increased from 2.9 eV to 3.0 eV (Fig. 3b). The increased bandgaps of S-CNNT and Pt-CNNT were derived from the change of in-plane units (Fig. 1b). These three different in-plane units made the long range ordered unit shorten, which would enlarge the bandgap due to the shorter in-plane ordered structure would cause quantum size effect. And the more blue PL peaks of S-CNNT and Pt-CNNT can also confirm it (Fig. 1c). In addition, the band tail absorption of S-CNNT and Pt-CNNT possess obvious reduction between 450 and 550 nm. Because the n-π^* transitions caused by the in-plane distortion were forbidden [14,26]. In Fig. 3b, the same bandgaps of S-CNNT and Pt-CNNT indicated the small and superficial Pt had no influence on the band structures of CNNT. However, absorption intensity of Pt-CNNT increased between 400 nm and 750 nm than S-CNNT (Fig. 3a), which originated from the semi-chemical interaction between Pt and CNNT increased state of density. In Fig. S5 (Supporting information), the digital images also proved the improved light absorption ability of Pt-CNNT.

As shown in Fig. 3c, S-CNNT possessed increscent photocurrent than CNNT, indicating the in-plane homojunction can accelerate the photogenerated charge migration. Furthermore, the photocurrent of Pt-CNNT boosted tremendously than S-CNNT, suggested the semi-chemical interaction between Pt and CNNT was more beneficial to charge migration. It was possibly because the semi-chemical interaction could reduce the energy barrier between Pt and CNNT. In Fig. 3d, S-CNNT possessed a longer PL lifetime than CNNT, and Pt-CNNT was similar to S-CNNT, which certified the homojunction could enhance the photogenerated charge separation, and then the Pt transferred the charge fast.

Photocatalytic activities of samples were evaluated by photocatalytic H_2 evolution test. As shown in Fig. S6 (Supporting information), Pt-CNNTs had ultrahigh photocatalytic H_2 evolution rate than Pt/CNNT and Pt/S-CNNT prepared by *in situ* photo-reduction of H_2PtCl_6. In order to compare the Pt utilization efficiency for H_2 evolution, the TOF was calculated according to H_2 evolution amount. As shown in Fig. 4a, the H_2 evolution TOF of Pt/S-CNNT had more than three times higher than Pt/CNNT, indicated the improved crystallinity and in-plane homojunction could enhance the photocatalytic activity of CNNT. As for Pt-CNNT, the H_2 evolution TOF reached up to 918 h^{-1}, and the enhancement factors were almost 63 and 200 times compared with that of Pt/S-CNNT and Pt/CNNT, respectively. Furthermore, the sizes of Pt NPs on Pt/CNNT and Pt-CNNT were similar (Fig. S7 in Supporting information), indicating the improved photocatalytic H_2 evolution activity was not caused by increased reduction sites amount. As shown in Fig. 4b, all of Pt-CNNTs showed the obvious boosting of H_2 evolution TOF, and the 0.05 wt% Pt decorated CNNT showed the highest TOF for H_2 evolution. In addition, the H_2 evolution TOF of Pt-CNNT was higher than that of most g-C_3N_4-based photocatalysts and even single-atom Pt decorated g-C_3N_4 reported previously (Fig. 4c) [16,19,28–40]. The drastic enhanced H_2 evolution TOF of Pt-CNNTs demonstrated that the semi-chemical interaction between Pt and CNNT was a subversive approach for efficient photocatalytic H_2 evolution. In addition, the photocatalytic H_2 evolution cycle test of Pt-CNNT showed excellent stability (Fig. S8 in Supporting information), which might be due to the strong interaction between Pt and CNNT.

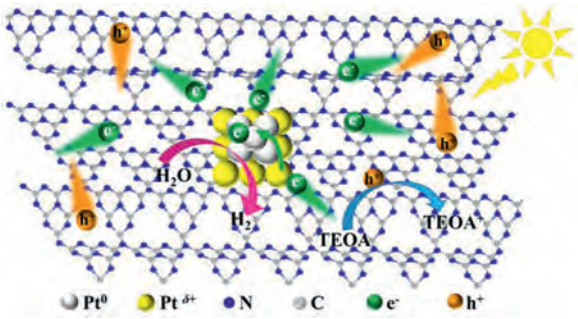

Fig. 5. Photocatalytic enhancement mechanism of Pt-CNNT.

Based on the above, the photocatalytic enhancement mechanism of Pt-CNNT was proposed in Fig. 5. Firstly, the increased crystallinity and in-plane homojunction could accelerate the photogenerated charge separation and restrain recombination; secondly, the strong interaction between Pt and CNNT made the charge transfer easier from CNNT to Pt by reducing the charge transfer barrier; thirdly, the superb H^+ reduction property of metallic Pt made the photo-induced electrons consumed rapidly for H_2 evolution. All of these were due to the semi-chemical interaction between Pt and CNNT from the solvothermal treatment.

In conclusion, a solvothermal method was developed to achieve the semi-chemical interaction between Pt and CNNT, at the same time, the in-plane homojunction of CNNT was formed. The semi-chemical interaction and in-plane homojunction in Pt-CNNT could reduce the charge transfer barrier, restrain the photogenerated charge recombination, accelerate H^+ reduction, and improve the charge separation and transfer. So, the Pt-CNNTs showed 200 times photocatalytic H_2 evolution TOF than that of Pt/CNNT, and the optimized sample showed the ultrahigh TOF of 918 h^{-1} under visible light ($\lambda > 420$ nm) irradiation, which is one of the highest in the g-C_3N_4-based photocatalysts. This work provided a subversive approach for efficient photocatalytic H_2 evolution.

Declaration of competing interest

The authors declare that they have no known competing financial interests or personal relationships that could have appeared to influence the work reported in this paper.

Acknowledgments

We gratefully acknowledge the financial support of the National Natural Science Foundation of China (Nos. 51868050, 51938007, 51878325, 51868052, 52100186, 52170082, and 52063024), the Natural Science Foundation of Jiangxi Province (Nos. 20202BAB213011 and 20181BBG78034) and the Scientific Research Foundation of Nanchang Hangkong University (No. EA201902377).

Supplementary materials

Supplementary material associated with this article can be found, in the online version, at doi:10.1016/j.cclet.2021.09.057.

References

[1] G.G. Zhang, X.C. Wang, Angew. Chem. Int. Ed. 58 (2019) 15580–15582.
[2] X.H. Jiang, L.S. Zhang, H.Y. Liu, et al., Angew. Chem. Int. Ed. 59 (2020) 23112–23116.
[3] X.L. Li, S.J. Song, Y.Q. Gao, et al., Small 17 (2021) 2101315.
[4] M. Faraji, M. Yousefi, S. Yousefzadeh, et al., Energy Environ. Sci. 12 (2019) 59–95.
[5] R. Shi, Y.H. Cao, Y.J. Bao, et al., Adv. Mater. 29 (2017) 1700803.
[6] Y.O. Wang, A. Vogel, M. Sachs, et al., Nat. Energy 4 (2019) 746–760.
[7] G.F. Liao, Y. Gong, L. Zhang, et al., Energy Environ. Sci. 12 (2019) 2080–2147.
[8] X.H. Jiang, F. Yu, D.S. Wu, et al., Chin. Chem. Lett. 32 (2021) 2782–2786.
[9] S Chen, T Hisatomi, M Nakabayashi, et al., Chem. Sci. 11 (2020) 6436–6441.
[10] M. Zhu, L.S. Zhang, S.S. Liu, et al., Chin. Chem. Lett. 31 (2020) 1961–1965.
[11] X. Li, J.G. Yu, M. Jaroniec, et al., Chem. Rev. 119 (2019) 3962–4179.
[12] J.D. Xiao, Q.C. Shang, Y.J. Xiong, et al., Angew. Chem. Int. Ed. 55 (2016) 1–6.
[13] M.J. Liu, P.F. Xia, L.Y. Zhang, et al., ACS Sustainable Chem. Eng. 6 (2018) 10472–10480.
[14] L.S. Zhang, N. Ding, M. Hashimoto, et al., Nano Res. 11 (2018) 2295–2309.
[15] Y. Qi, Y. Zhao, Y.Y. Gao, et al., Joule 2 (2018) 2393–2402.
[16] W.N. Xing, W.G. Tu, M. Ou, et al., ChemSusChem 12 (2019) 2029–2034.
[17] Y.N. Wang, L.N. Guo, Y.Q. Zeng, et al., ACS Appl. Mater. Interfaces 11 (2019) 30673–30681.
[18] L.S. Zhang, N. Ding, L.C. Lou, et al., Adv. Funct. Mater. 29 (2019) 1806774.
[19] X.G. Li, W.T. Bi, L. Zhang, et al., Adv. Mater. 28 (2016) 2427–2431.
[20] H. Su, W. Che, F.M. Tang, et al., J. Phys. Chem. C 122 (2018) 21108–21114.
[21] M.H. Sun, J.P. Ji, M.Y. Hu, et al., ACS Catal. 9 (2019) 8213–8223.
[22] Y.C. Nie, F. Yu, L.C. Wang, et al., Appl. Catal. B: Environ. 227 (2018) 312–321.
[23] X.S. Wang, C. Zhou, R. Shi, et al., Nano Res. 12 (2019) 2385–2389.
[24] L.H. Lin, H.H. Ou, Y.F. Zhang, et al., ACS Catal. 6 (2016) 3921–3931.
[25] H. Wang, X.S. Sun, D.D. Li, et al., J. Am. Chem. Soc. 139 (2017) 2468–2473.
[26] Y. Chen, B. Wang, S. Lin, et al., J. Phys. Chem. C 118 (2014) 29981–29989.
[27] Z.X. Zeng, H.T. Yu, X. Quan, et al., Appl. Catal. B: Environ. 227 (2018) 153–160.
[28] Y. Zheng, L.H. Lin, X.J. Ye, et al., Angew. Chem. Int. Ed. 53 (2014) 11926–11930.
[29] G.G. Liu, G.X. Zhao, W. Zhou, et al., Adv. Funct. Mater. 26 (2016) 6822–6829.
[30] Q. Han, B. Wang, J. Gao, et al., ACS Nano 10 (2016) 2745–2751.
[31] P. Niu, L.L. Zhang, G. Liu, et al., Adv. Funct. Mater. 22 (2012) 4763–4770.
[32] D.J. Martin, K.Q. Qiu, S.A. Shevlin, et al., Angew. Chem. Int. Ed. 53 (2014) 9240–9245.
[33] M.K. Bhunia, K. Yamauchi, K. Takanabe, Angew. Chem. Int. Ed. 53 (2014) 11001–11005.
[34] S.B. Yang, Y.J. Gong, J.S. Zhang, et al., Adv. Mater. 25 (2013) 2452–2456.
[35] J.S. Zhang, M.W. Zhang, C. Yang, et al., Adv. Mater. 26 (2014) 4121–4126.
[36] Z.Z. Lin, X.C. Wang, Angew. Chem. Int. Ed. 52 (2013) 1735–1738.
[37] H. Xu, J.J. Yi, X.J. Xie, et al., Appl. Catal. B: Environ. 220 (2018) 379–385.
[38] J.H. Sun, J.S. Zhang, M.W. Zhang, et al., Nat. Commun. 3 (2012) 1139.
[39] Y.D. Hou, A.B. Laursen, J.S. Zhang, et al., Angew. Chem. Int. Ed. 52 (2013) 3621–3625.
[40] X.J. She, J.J. Wu, J. Zhong, et al., Nano Energy 27 (2016) 138–146.